

## Energy Relaxation Time between Macroscopic Quantum Levels in a Superconducting Persistent-Current Qubit

Yang Yu, D. Nakada, Janice C. Lee, Bhuwan Singh, D. S. Crankshaw, T. P. Orlando, and Karl K. Berggren  
*Massachusetts Institute of Technology, Cambridge, Massachusetts 02139, USA*

William D. Oliver

*MIT Lincoln Laboratory, Lexington, Massachusetts 02420, USA*  
(Received 28 October 2003; published 18 March 2004)

We measured the intrawell energy relaxation time  $\tau_d \approx 24 \mu\text{s}$  between macroscopic quantum levels in the double well potential of a Nb persistent-current qubit. Interwell population transitions were generated by irradiating the qubit with microwaves. Zero population in the initial well was then observed due to a multilevel decay process in which the initial population relaxed to lower energy levels during the driven transitions. The decoherence time, estimated from  $\tau_d$  within the spin-boson model, is about  $20 \mu\text{s}$  for this configuration with a Nb superconducting qubit.

DOI: 10.1103/PhysRevLett.92.117904

PACS numbers: 03.67.Pp, 03.65.Yz, 85.25.Cp, 85.25.Dq

Recent successes with superconducting qubits (SQs) have enhanced the feasibility of implementing quantum computing (QC) with Josephson devices [1–9]. Rabi oscillations, which are a preliminary requirement of QC, have been reported in charge, phase, and flux qubits [3–8]. However, the systematic experimental investigation of decoherence, which is a key issue for SQs, is sparse so far due to the challenge of the time resolution of the measurement. Although long decoherence times have been demonstrated in some special configurations [4,5,8,10], the limiting source of decoherence in the SQs remains unidentified. On the other hand, the decoherence time for SQs, including energy and phase relaxation times, is predicted to be proportional to the level of dissipation, which results from the coupling between the qubits and the environment [11,12]. Therefore, quantifying the dissipation is extremely useful in the design of qubits from various new materials, because it indicates whether the dissipation is at least low enough to make error-tolerant QC feasible. Previous methods to determine the dissipation of devices are either applicable at relatively high temperatures [10] or rely on indirect measurements of switching probabilities [13]. In addition, all long decoherence times ( $\sim 1 \mu\text{s}$ ) reported have been obtained in NbN and Al SQs [4,5,8,10]. It is important to know whether a promising decoherence time can be achieved in Nb-based SQs, which has a more mature fabrication capability. In this Letter, we present time-resolved measurements of the intrawell relaxation time  $\tau_d$  in a Nb persistent-current (PC) qubit. We found that  $\tau_d \approx 24 \mu\text{s}$ . The corresponding phase-decoherence time within a spin-boson model (SBM) is inferred to be longer than  $20 \mu\text{s}$ . These long decoherence times indicate a strong potential for QC employing Nb-based SQs.

A PC qubit is a superconducting loop broken by three underdamped Josephson junctions (JJs) [Fig. 1(a)]. Two JJs are designed to have the same critical current, and the third one is designed to be  $\alpha$  times smaller. For  $0.5 <$

$\alpha < 1$  and with an externally applied magnetic field close to a half-flux quantum  $\Phi_0/2$ , the system is analogous to a particle in a two-dimensional potential well with eigenenergies calculated in Ref. [14]. However, the lowest relevant states effectively reflect a particle in a one-dimensional double-well potential with quantized energy levels shown in Fig. 1(b), and whose classical states in each well correspond to macroscopic persistent currents of opposite sign [15]. The potential shown in Fig. 1(b) can be tilted by changing the frustration  $f_q$ , the magnetic flux threading the loop in units of  $\Phi_0$ . The two classical states are coupled via quantum tunneling through the barrier between the wells. In addition, the system can interact with a monochromatic electromagnetic (microwave) field, and microwaves with frequency matching the energy level spacing can generate transitions between the two macroscopic quantum states, namely, photon-induced transitions (PITs) [2,8].

The samples used in this study were fabricated at MIT Lincoln Laboratory in a Nb trilayer process [16]. The critical current density is  $J_c \sim 370 \text{ A/cm}^2$ . The critical currents of the large and small JJs in the qubit, determined from thermal activation studies [17], are  $I_c \approx 1.2$  and  $0.75 \mu\text{A}$ , respectively ( $\alpha \approx 0.63$ ). The qubit energy

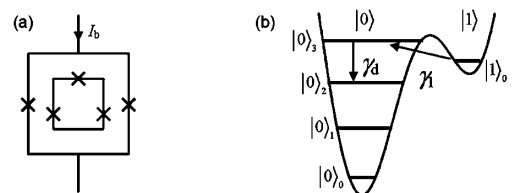


FIG. 1. (a) Schematic of the PC qubit surrounded by a readout dc SQUID. (b) Schematic of the qubit's double-well potential with energy levels for an applied frustration close to  $0.485\Phi_0$ . Microwaves pump the qubit from the lowest level of  $|1\rangle$  ( $|1\rangle_0$ ) to the third excited level of  $|0\rangle$  ( $|0\rangle_3$ ), then decay to the second excited level of  $|0\rangle$  ( $|0\rangle_2$ ) with a rate  $\gamma_d$ .

level structure calculated using qubit parameters is shown in Fig. 2 of Ref. [14]. The persistent current in the qubit loop can be read out by a dc SQUID which surrounds the qubit. For our device parameters [14,17], the persistent current will generate an additional magnetic flux of  $\sim 3 m\Phi_0$  in the SQUID, resulting in a  $0.3 \mu\text{A}$  change in the switching current  $I_{\text{sw}}$  of the SQUID that can be easily detected at  $T < 50 \text{ mK}$ . The sample was mounted on a chip carrier that was enclosed in an oxygen-free-copper sample cell and thermally anchored to the mixing chamber (MC) of a dilution refrigerator. The devices were magnetically shielded by four cryoperm-10 cylinders surrounding the inner vacuum can. All electrical leads that connected the SQUID to room temperature electronics were carefully filtered by electromagnetic interference filters (at 300 K), RC filters (at 1.6 K), and copper powder filters (at 15 mK). Microwaves were injected to the qubit via a separate semirigid cryogenic coaxial cable with 20 dB attenuators at the 1 K pot and the MC. Battery-powered low-noise preamplifiers were used for all measurements. The diagnostic tests performed on JJs indicated that there was no significant extrinsic noise in our system.

Spectroscopy of the qubit energy levels was achieved using microwave pulses to produce PITs. For each measurement trial (Fig. 2), we first prepared the qubit in state  $|1\rangle$  by tilting the potential (i.e., applying frustration) to a regime where the system has a single well and then waiting a sufficiently long time. After the qubit had relaxed to its ground state, the potential was tilted back to the frustration where it was to be measured. At low temperatures, the qubit will have a finite probability of remaining in  $|1\rangle$ , which is effectively metastable on the time scales considered in this Letter. We then applied microwaves with duration time  $t_{\text{pul}}$ , inducing transitions between states  $|1\rangle$  and  $|0\rangle$ . After the microwaves were shut off, the bias current of the SQUID was ramped through values slightly higher than its critical current  $I_{c0}$ . The qubit state ( $|0\rangle$  or  $|1\rangle$ ) was then read out from the current at which the SQUID switched to a finite voltage state [ $\mathbf{0}$  or  $\mathbf{1}$  in Fig. 2(d)]. For a fixed frustration, this procedure was repeated more than  $10^3$  times to minimize the statistical error. A histogram of  $I_{\text{sw}}$  clearly shows the probability distribution of the qubit state occupation. Shown in Fig. 3 are contour plots of the switching-current histograms obtained by scanning the frustration at  $T = 15 \text{ mK}$ . Each vertical slice is a histogram of  $I_{\text{sw}}$ , and the color represents the number of switching events (proportional to the switching probability). A bimodal structure in the switching-current distribution, caused by the opposite persistent current of the qubit, was observed at  $f_q \sim 0.485\Phi_0$ . The lower branch represents the qubit in the  $|0\rangle$  state, and the upper branch represents the qubit in the  $|1\rangle$  state. The substantial population in state  $|1\rangle$  demonstrates that we had successfully prepared the qubit in  $|1\rangle$ , because, near  $f_q \sim 0.485\Phi_0$ , the qubit had a much higher single-well ground-state energy in  $|1\rangle$  than that in  $|0\rangle$ .

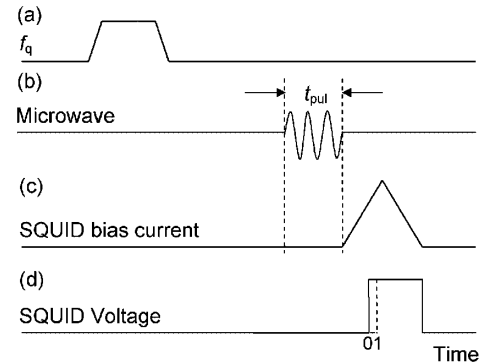


FIG. 2. Time profiles of (a) bias frustration, (b) microwave amplitude, (c) SQUID bias current, and (d) SQUID voltage for one measurement trial.  $\mathbf{0}$  and  $\mathbf{1}$  indicate that the qubit states ( $|0\rangle$  or  $|1\rangle$ ) result in different  $I_{\text{sw}}$ .

However, the energy barrier height and width relative to the lowest energy level of state  $|1\rangle$ , denoted as  $|1\rangle_0$ , were small enough so that the qubit had a large probability of tunneling to  $|0\rangle$ . The leftmost tip of the higher branch marked a fixed frustration point  $f_q \approx 0.484\Phi_0$ , below which it was impossible for the qubit to stay in  $|1\rangle$ , because the potential becomes essentially a single-well  $|0\rangle$  state. Microwaves, with frequencies matching the energy difference between  $|1\rangle_0$  and one of the levels of  $|0\rangle$ , were used to generate transitions between states  $|1\rangle$

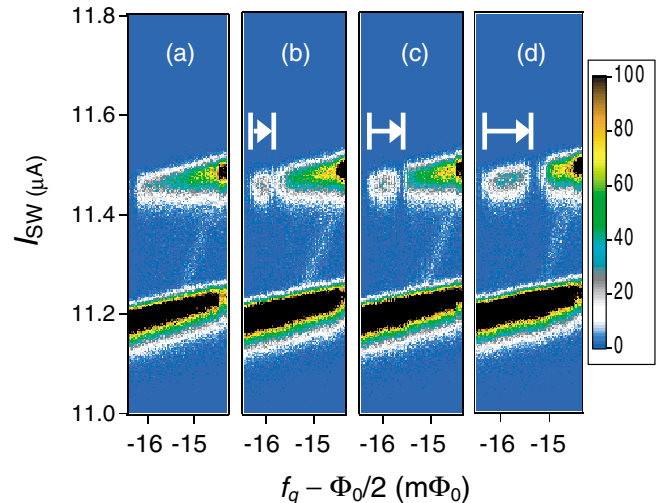


FIG. 3 (color). Contour plots of the switching current distribution (a) without microwaves and with microwaves at (b)  $\nu = 6.77$ , (c)  $7.9$ , and (d)  $9.66 \text{ GHz}$ . In each plot, the leftmost tip of the upper branch corresponds to a fixed frustration point  $f_q \approx 0.484\Phi_0$ . Without microwave irradiation, the population in the upper branch (state  $|1\rangle$ ) decreased continuously to zero as the frustration decreased from  $\Phi_0/2$ . Microwaves pumped the population from state  $|1\rangle$  to state  $|0\rangle$  at the resonant frustration, the bias point at which the microwave frequency matched the energy level spacing between two states. The white arrows indicate that the resonant frustration moves toward  $\Phi_0/2$  with increasing microwave frequency, in agreement with the qubit energy structure [Ref. [14]].

and  $|0\rangle$ . The most striking feature of the contour plots is that a population “gap” (i.e., zero population region) in the  $|1\rangle$  branch was created by the microwaves [Figs. 3(b)–3(d)]. With increasing microwave frequency, the gap moved away from the tip, as expected from the energy level structure [Ref. [14]]. The quantitative agreement between the gap position and the energy level structure confirmed that the gap resulted from the microwave PIT between the two macroscopic quantum states  $|1\rangle_0$  and  $|0\rangle_3$  (the third excited energy level of the state  $|0\rangle$ ). We believe that the PIT here was an incoherent process, because the microwave pulse duration was  $600\ \mu\text{s}$ , much longer than the estimated decoherence time ( $0.1\text{--}100\ \mu\text{s}$ ) [2,8,15]. Additionally, no periodic variation of population with varying pulse duration (for long pulses) was observed. In a simple two-level system, observing such a gap would be unexpected for an incoherent transition, since the population in the lower level ( $|1\rangle_0$ ) should always be larger than 0.5 in that case [18]. In order to address this gap phenomenon in our multilevel system, a multilevel pump-decaying model is introduced.

For simplicity we considered only three levels, the initial state  $|1\rangle_0$ , the  $|0\rangle_3$  state to which radiation induces a transition, and the state  $|0\rangle_2$  to which the population of  $|0\rangle_3$  decays. More accurately, the state  $|0\rangle_3$  decays to  $|0\rangle_2$ ,  $|0\rangle_1$ , and  $|0\rangle_0$ , but, for ease of calculation, we collectively label these states as  $|0\rangle_2$  with an overall effective intrawell decay rate  $\gamma_d \equiv 1/\tau_d$ . The temporal evolution of the three-level system under microwave irradiation is thereby described by the following three coupled rate equations:

$$\frac{dP_{10}}{dt} = -\gamma_1 P_{10} + (\gamma_1 + \gamma_2) P_{03}, \quad (1)$$

$$\frac{dP_{03}}{dt} = \gamma_1 P_{10} - (\gamma_1 + \gamma_2) P_{03} - \gamma_d P_{03}, \quad (2)$$

$$\frac{dP_{02}}{dt} = \gamma_d P_{03}, \quad (3)$$

in which  $P_{10}$ ,  $P_{03}$ , and  $P_{02}$  are the occupation probabilities of levels  $|1\rangle_0$ ,  $|0\rangle_3$ , and  $|0\rangle_2$ , respectively.  $\gamma_1$  is the stimulated transition rate between  $|1\rangle_0$  and  $|0\rangle_3$ , and  $\gamma_2$  is the spontaneous relaxation rate from  $|0\rangle_3$  to  $|1\rangle_0$ . Generally, for a given system,  $\gamma_1$  is proportional to the microwave power  $P_{\text{rf}}$ , and  $\gamma_2$  can be considered to be a constant [18]. For the initial condition  $P_{10}(0) = 1$ , with  $P_{03}(0) = P_{02}(0) = 0$ , Eqs. (1)–(3) can be solved analytically. For  $\gamma_1 \gtrsim \gamma_d$ , which is satisfied in our experiment, the probability of finding the qubit remaining in the state  $|1\rangle_0$  at  $t > 1/(2\gamma_1 + \gamma_2 + \gamma_d)$  is given by

$$P_{10}(t) \approx a_1 e^{-t/\tau'}, \quad (4)$$

where  $a_1$  depends weakly on the microwave power and can be considered as a constant in the relevant time scale,

$$\tau' \approx (2 + \gamma_2/\gamma_1)\tau_d = (2 + \gamma_2/AP_{\text{rf}})\tau_d, \quad (5)$$

and  $A$  is the coupling constant between the microwave source and the qubit. The physical picture of the three-level pump-decaying process is that microwaves

populate the highest level with a population  $P_{03} \propto 1/(2 + \gamma_2/\gamma_1)$ , which decays to the lowest level with a rate  $\gamma_d$ . Therefore, the effective decay rate of the population of the initial state is given by Eq. (5), and with  $t$  sufficiently long,  $P_{10}(t) \rightarrow 0$ ; this agrees with the experimental observations.

A significant impact of Eqs. (4) and (5) is that  $\tau_d$  can be determined by measuring  $P_{10}(t)$ . Because  $I_{\text{sw}}$  of  $|0\rangle$  is smaller than that of  $|1\rangle$ , pumping the system from state  $|1\rangle$  to state  $|0\rangle$  will generate a dip in the  $I_{\text{sw}}$  average as a function of frustration, and the dip amplitude is proportional to  $1 - P_{10}$ . Figure 4 shows the dip amplitude as a function of the microwave irradiation time  $t_{\text{pul}}$ . The nominal power of the microwave source was  $P_{\text{rf}} = 31.3\ \mu\text{W}$ . The time constant  $\tau'$ , obtained from a best fit, is  $130 \pm 20\ \mu\text{s}$ . We emphasize that  $\tau'$  is not equal to  $\tau_d$ , but, rather, it depends on  $\gamma_2/\gamma_1$ . For large  $P_{\text{rf}}$  (i.e.,  $\gamma_1 \gg \gamma_2$ ),  $\tau'$  will saturate to  $2\tau_d$ . For  $\gamma_1 \sim \gamma_2$ , we are able to determine  $\tau_d$  by measuring the  $P_{\text{rf}}$  dependence of  $\tau'$ . Shown in Fig. 5 is  $\tau'$  measured at various  $P_{\text{rf}}$ .  $\tau'$  saturates at about  $50\ \mu\text{s}$  for  $P_{\text{rf}} > 0.2\ \text{mW}$ . By adjusting  $\gamma_2/A$  and  $\tau_d$  as fitting parameters, we obtained  $\tau_d \approx 24.3 \pm 2.7\ \mu\text{s}$  from a best fit to Eq. (5), which is consistent with dc tunneling spectroscopy measurements [14]. This long intrawell energy relaxation time is of the same order of magnitude as the reported energy relaxation times in NbN and Al-based qubits [4,5,8,10]. Note that  $\gamma_2$  is another important parameter which determines interwell energy relaxation. Unfortunately, we could not directly extract  $\gamma_2$  from the fitting, because we do not know the coupling constant  $A$ . Future experiments in which microwave coupling is independently characterized should allow the extraction of  $\gamma_2$ .

The primary effect of the environmental dissipation on the intrawell dynamics of the PC qubits is that, at low temperature ( $k_B T \ll$  level spacing), the width of an excited level with energy  $E_n$  is given approximately by  $\gamma_d \approx E_n/Q$ , where  $Q$  is the quality factor of the classical small

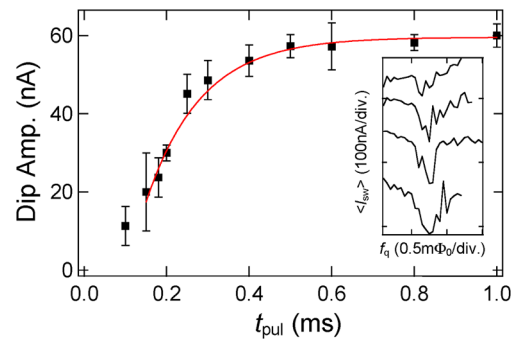


FIG. 4 (color online). The amplitude of the microwave resonant dip as a function of microwave duration  $t_{\text{pul}}$ . The microwave frequency  $\nu = 9.66\ \text{GHz}$  and nominal power  $P_{\text{rf}} = 31.3\ \mu\text{W}$ . The solid squares are experimental data and the line is a best fit to an exponential decay. The inset shows the resonant dips at  $t_{\text{pul}} = 0.2, 0.5, 0.8,$  and  $1\ \text{ms}$ , from top to bottom.

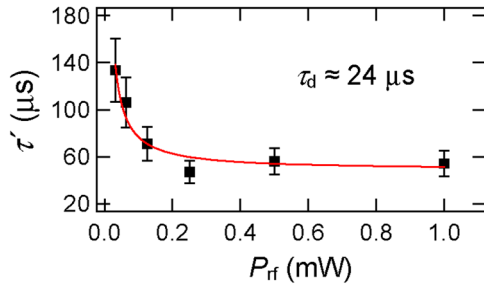


FIG. 5 (color online).  $\tau'$  vs microwave power for  $\nu = 9.66$  GHz. The solid line is a best fit to Eq. (5).

oscillation in the potential well [19]. From  $\tau_d$  we determined  $Q \sim 5 \times 10^5$ , close to the value obtained from thermal activation measurements at intermediate temperatures 0.3–1.2 K [17]. Note that  $Q$  is proportional to the subgap resistance, which ideally depends on the temperature as  $\sim e^{\Delta_s/k_B T}$  [20], where  $\Delta_s$  is the superconducting gap voltage. The temperature independence of  $Q$  suggests the presence of additional environmental sources of dissipation [15].

This long intrawell relaxation time is important for experiments in QC in two ways. First, the lower two energy levels in the left well,  $|0\rangle_0$  and  $|0\rangle_1$ , could themselves be used as the two qubits states, with a third state  $|0\rangle_3$  used as the readout state. Because our PC qubit had no leads directly connected to it and the magnetic coupling circuit is optimally designed to lessen the effects of the electromagnetic environment, the PC qubit is much less influenced by this environment than are other similar single-junction schemes [5,6,9]. Second, if we assume that the environment can be modeled as an Ohmic bath, as in the SBM, then we can estimate the decoherence times of a PC qubit in which the qubit states are those of opposite circulating current [2,8,15]. The energy relaxation and phase-decoherence times are given in the SBM for an Ohmic environment by [11]

$$\tau_{\text{relax}}^{-1} \approx \pi \alpha_L \sin^2 \eta \Delta E / \hbar, \quad (6)$$

$$\tau_{\varphi}^{-1} = \tau_{\text{relax}}^{-1} / 2 + 2\pi \alpha_L k_B T \cos^2 \eta / \hbar, \quad (7)$$

where  $\Delta E$  is the energy difference between levels in opposite wells,  $\eta \approx \text{tg}^{-1}(\Delta/\Delta E)$  is the mixing angle,  $\Delta$  is the tunneling amplitude between the wells, and  $\alpha_L \sim 1/Q$  is the quantum damping parameter [19] which we estimate using our measured  $Q$  value. For our Nb PC qubit operating with opposite circulating currents states (for instance, biased near  $f_q \approx 0.485\Phi_0$ , where  $\Delta \approx 2$  GHz and  $\Delta E \approx 4$  GHz), a conservative estimate gives  $\tau_{\text{relax}} \gtrsim 30 \mu\text{s}$  and  $\tau_{\varphi} \gtrsim 20 \mu\text{s}$  at 15 mK. We emphasize that an Ohmic environment model may not adequately describe all sources of decoherence; these times must be viewed as estimates pending experimental verification. Nonetheless, for a typical Rabi frequency  $\Omega = 1$  GHz,

we obtained a quantum quality factor  $> 10^4$ , larger than the oft-quoted basic requirement for error-tolerant QC. Considering the attractiveness of Nb-based SQs from the point of view of robust and well-developed fabrication methods, these times indicate that they are a promising candidate for realizing a scalable quantum computer.

In summary, we directly measured the intrawell relaxation time of a Nb-based PC qubit by generating PITs between macroscopically distinct quantum states. A multilevel decay process was observed with an intrawell relaxation time of about 24  $\mu\text{s}$  and a  $Q$  factor of greater than  $10^5$ , indicating that these intrawell levels are well isolated from the environment and are themselves a good qubit candidate. Likewise, these measurements suggest that the flux qubits operating between wells could also have sufficient decoherence times, demonstrating good prospects for well-fabricated Nb junctions, with their more mature technology, to be used as SQs.

We thank K. Segall, B. Cord, D. Berns, and A. Clough for technical assistance and S. Valenzuela, M. Tinkham, L. Levitov, and M. Vavilov for helpful discussions. This work was supported by AFOSR Grant No. F49620-01-1-0457 under the DURINT program and by ARDA. The work at Lincoln Laboratory was sponsored by the U.S. DOD under the Air Force, Contract No. F19628-00-C-0002.

- 
- [1] J.R. Friedman *et al.*, Nature (London) **406**, 43 (2000).
  - [2] C.H. van der Wal *et al.*, Science **290**, 773 (2000).
  - [3] Y. Nakamura, Y.A. Pushkin, and J.S. Tsai, Nature (London) **398**, 786 (1999).
  - [4] D. Vion *et al.*, Science **296**, 886 (2002).
  - [5] Y. Yu *et al.*, Science **296**, 889 (2002).
  - [6] J.M. Martinis *et al.*, Phys. Rev. Lett. **89**, 117901 (2002).
  - [7] Y.A. Pashkin *et al.*, Nature (London) **421**, 823 (2003).
  - [8] I. Chiorescu *et al.*, Science **299**, 1869 (2003).
  - [9] A.J. Berkley *et al.*, Science **300**, 1548 (2003).
  - [10] S. Han *et al.*, Science **293**, 1457 (2001).
  - [11] A.J. Leggett *et al.*, Rev. Mod. Phys. **59**, 1 (1987); Y. Makhlin, G. Schön, and A. Shnirman, Rev. Mod. Phys. **73**, 357 (2001).
  - [12] W.H. Zurek, Phys. Today **44**, No. 10, 36 (1991).
  - [13] C. Cosmelli *et al.*, Phys. Rev. Lett. **82**, 5357 (1999); S. Han and R. Rouse, Phys. Rev. Lett. **86**, 4191 (2001).
  - [14] D.S. Crankshaw *et al.*, Phys. Rev. B (to be published).
  - [15] T.P. Orlando *et al.*, Phys. Rev. B **60**, 15398 (1999).
  - [16] K.K. Berggren *et al.*, IEEE Trans. Appl. Supercond. **9**, 3271 (1999).
  - [17] K. Segall *et al.*, Phys. Rev. B **67**, 220506 (2003).
  - [18] D.J. Griffiths, *Introduction to Quantum Mechanics* (Prentice-Hall, Englewood Cliffs, NJ, 1995), p. 311.
  - [19] J.M. Schmidt, A.N. Cleland, and J. Clarke, Phys. Rev. B **43**, 229 (1991); W. Bialek, S. Chakravarty, and S. Kivelson, Phys. Rev. B **35**, 120 (1987).
  - [20] P. Silvestrini *et al.*, Phys. Rev. Lett. **60**, 844 (1988).